SCIENTIFIC REPORTS

OPEN

SUBJECT AREAS:
OPTICAL MATERIALS
SENSORS
COORDINATION CHEMISTRY
METAL-ORGANIC FRAMEWORKS

Received
11 August 2014

Accepted
12 September 2014

Published
1 October 2014

Correspondence and requests for materials should be addressed to M.O. (moh@yonsei.ac.kr)

Highly effective heterogeneous chemosensors of luminescent silica@coordination polymer core-shell micro-structures for metal ion sensing

Won Cho, Hee Jung Lee, Sora Choi, Yoona Kim & Moonhyun Oh

Department of Chemistry, Yonsei University, 134 Shinchon-dong, Seodaemun-gu, Seoul 120-749, Korea.

Heterogeneous solid sensors are regarded as promising next-generation sensor due to their excellent chemical stability, low contamination, and excellent recyclability, despite their low sensitivity and weak signal. The dispersity and signals specifically from the exterior of solid sensors are critical aspects which define the sensing sensitivity and selectivity. A novel strategy for the preparation of ideal heterogeneous sensors based upon luminescent lanthanide coordination polymers (LnCP) has been demonstrated. Ideal heterogeneous sensors are systematically achieved by producing the sensors in small, uniform, and thin core-shell particles (silica@LnCP, Ln = Eu, Tb). Eventually, we found that the extremely small amount of well-structured silica@LnCP microsphere, less than *ca.* 1/400 compared to the amount of several known coordination polymer-based sensors, was sufficient to achieve a reliable Cu^{2+} sensing with even much greater sensitivity (*ca.* 550% improvement).

The effective detection of small amounts of metal ions is important in many environmental and biological systems. In special, the detection of Cu^{2+} is essential in biological systems, as Cu^{2+} plays vital roles for living organisms. Wilson's disease and Alzheimer's disease are two known examples related to alterations in Cu^{2+} cellular homeostasis[1,2]. Recent developments in Cu^{2+} sensing methodology include discrete molecular chemosensor systems and heterogeneous solid sensing materials[3–6]. In general, homogeneous sensors based upon discrete molecules show more effective sensing events than heterogeneous solid sensors, which exhibit low sensitivity and weak signals. However, there is great demand for heterogeneous solid sensors due to their excellent chemical stability, low contamination, and excellent recyclability. Therefore, the development of effective solid sensor materials remains an important and challenging area. Coordination polymers (CPs) or metal-organic frameworks (MOFs) are fascinating materials for use in heterogeneous solid sensors because their compositions and properties can be easily tuned by altering their components, metal ions or organic building blocks[6–16]. Lanthanide-based MOFs (LnMOFs) or lanthanide-based CPs (LnCPs), including EuMOFs and TbMOFs, have been extensively investigated as luminescent sensor materials. They showed great ability in the sensing process due to their sharp and strong emissions and long luminescent lifetimes originating from characteristic f-f transitions[8–16]. It should be noted that CPs and MOFs are widely used in a variety of applications in addition to sensing, such as gas storage, gas separation, and catalysis[17–24].

The luminescent intensity of LnMOFs (including LnCPs) is typically altered depending upon the identity of analytes through analyte-metal or analyte-ligand interactions. Though several LnMOFs have been developed as luminescent sensor materials to detect metal ions, anions, or small molecules[8–16], the majority of these were prepared in the form of bulk macro-scaled materials. During sensing events of heterogeneous solid sensors, signals from exterior of the sensor materials rather than those from interior of materials should be more critical to define the sensing sensitivity and selectivity. Therefore, the systematic decrease in the size of sensor materials will be a critical factor in sensing enhancement and reducing material cost. On the other hands, several research groups, including our group, have recently developed nano- and micro-sized coordination polymer particles (CPPs) or MOFs[25–30]. The development of CPPs or nano-MOFs enhanced their original properties and extended their application range[27–30]. Herein, we report highly effective heterogeneous sensor materials made from luminescent lanthanide(III) coordination polymers (LnCP) in the form of simple microspheres or core-shell microspheres. We found that the inside of solid sensor materials was not important for the effective sensing process.

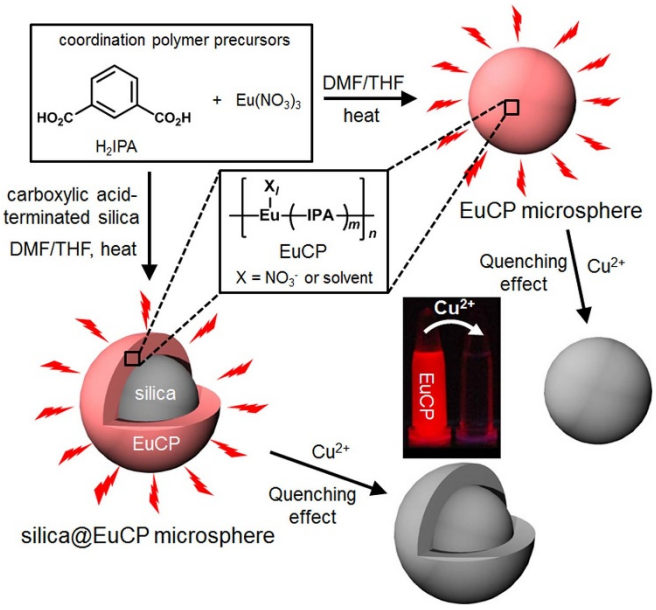

Figure 1 | Synthesis and sensing process of EuCP and silica@EuCP microspheres. Schematic representation of luminescent sensors of micro-sized EuCP and silica@EuCP core-shell structures.

Sensor materials were lightened through making those in the form of small core-shells with thin sensing shell. Eventually, only less than ~ 1/400 of core-shell typed LnCP microspheres, compared to typical LnMOF-based or LnCP-based sensor materials, was required to achieve a reliable sensing process, and this exceptionally small amount of LnCP even showed a higher sensitivity on metal ion detection. The excellent recycling capability of the resulting micro-sized core-shell type sensor was also demonstrated.

Results

Synthesis of luminescent EuCP microspheres. Luminescent spherical particles made from europium(III) coordination polymer (EuCP) were rapidly and conveniently synthesized *via* the simple solvothermal reaction of coordination polymer precursors containing $Eu(NO_3)_3$ and isophthalic acid (H_2IPA) at 140°C for 20 min (Fig. 1). It should be noted that a considerable process time (1 ~ 3 days) is typically required for the preparation of LnMOF-based sensor materials[8–13]. The isolated EuCP microspheres were characterized using scanning electron microscopy (SEM), scanning transmission electron microscopy (STEM), confocal microscopy, powder X-ray diffraction (PXRD), energy dispersive X-ray (EDX), infrared (IR), and emission spectroscopy. The formation of spherical particles with an average size of 0.70 ± 0.06 μm was first identified from SEM and STEM images (Fig. 2a). The chemical composition of EuCP microspheres was determined *via* EDX spectrum, where carbon, oxygen, and europium atoms were detected (Fig. 2b). The shift of the CO stretching frequency to 1606 cm^{-1} in the IR spectrum of EuCP microspheres from 1692 cm^{-1} for uncoordinated H_2IPA revealed the coordination of the carboxylate groups of IPA to Eu^{3+} ions (Supplementary Fig. S1). Featureless PXRD pattern of EuCP microspheres revealed that they are amorphous and not crystalline materials, and so the structural details on those materials cannot be obtained (Supplementary Fig. S2a). Finally, the emission spectrum of EuCP microspheres showed the characteristic transitions of Eu^{3+} ions (Fig. 2d). The strong emission bands at 592 and 615 nm are related to the $^5D_0 \rightarrow {}^7F_1$ and $^5D_0 \rightarrow {}^7F_2$ transitions of Eu^{3+} ions, respectively[8–10]. These intense transitions resulted in the red emission of particles. The confocal microscopy image (Fig. 2c) and the photograph in the presence of UV irradiation (inset in Fig. 2d) of EuCP microspheres visually showed the luminescence in red regions of the spectrum. The weak emission bands at 651 and 698 nm originating from the $^5D_0 \rightarrow {}^7F_3$ and $^5D_0 \rightarrow {}^7F_4$ transitions were also observed in the emission spectrum.

Selective Cu^{2+} sensing of luminescent EuCP microspheres. The utilization of EuCP microspheres as a luminescent sensor for metal ion detection was then investigated. The excellent dispersity of heterogeneous solid sensor materials in solution is a vital prerequisite for the sensitive and reliable detection of analytes. Within this point, the resulting EuCP microspheres, which exhibit an excellent dispersity in the solution (see insets in Fig. 2c,d), should be an excellent candidate for the heterogeneous solid sensor and should exhibit superior properties when compared to typical bulk-scaled MOF-based sensor materials. Note that an extra grind process of bulk MOFs was generally required for their utilization as a sensor in solution; this process may not be sufficient to achieve an excellent dispersity[13,14]. The titration of well-dispersed MeCN suspensions of EuCP microspheres with various concentrations of Cu^{2+} revealed a decrease in the luminescent intensity of EuCP microspheres with increasing amounts of added-Cu^{2+} (Fig. 2d). Interestingly, we found that quite a small amount of sensor materials (EuCP, 0.1 mg) was required during the sensing process, compared to the archetypal quantities of bulk MOF-based sensing materials at *ca.* 1 ~ 10 mg (Table 1)[8–13]. This reduction in the amount of sensor materials required during a sensing event is possibly due to the small size and excellent dispersity of the EuCP microspheres. Luminescent turn-off sensing on Cu^{2+} of EuCP microspheres was also easily recognized by the naked eye, as shown in inset of Fig. 2d. The initial strong red emission of the EuCP microspheres almost disappeared after interaction with Cu^{2+}. The decrease in emission bands could stem from the quenching effect attributed to the interaction of Cu^{2+} with coordination polymers. Specifically, the interaction of Cu^{2+} with a Lewis base within materials is a well-established quenching process[10–13], and the oxygen atom of the carboxylate group is known as one example of a Cu^{2+} ion interacting site[8,9]. In addition, the Cu^{2+}-detecting sensitivity of EuCP microspheres was significantly higher than the many known LnMOF-based sensor materials (Table 1)[8–13]. The quantified value of the quenching effect of Cu^{2+} was obtained using the Stern-Volmer equation ($I_0/I = 1 + K_{sv}[M]$)[9–11]. The quenching effect coefficient K_{sv} value (12,485 M^{-1}) of EuCP microspheres for Cu^{2+} ions exhibited more than ~ 200% improvement over many known LnMOF-based sensor materials (Table 1)[8–13].

The selectivity of EuCP microspheres on Cu^{2+} sensing was certified through observation of parallel reactions using various other metal ions instead of Cu^{2+}. Luminescent EuCP microspheres were immersed in various MeCN solutions (5 mM) containing different kinds of metal ions, such as Mn^{2+}, Co^{2+}, Ni^{2+}, Zn^{2+}, Cd^{2+}, Mg^{2+}, Ca^{2+}, and Ag^{+}. Changes in the luminescent intensity of the initial EuCP microspheres were quite different depending upon the specific type of metal ions. As shown in Fig. 2e,f, significant change in luminescent intensity was only observed when EuCP microspheres were immersed in Cu^{2+} solution. Alkaline-earth metal ions (Mg^{2+} and Ca^{2+}) and other transition metal ions (Mn^{2+}, Co^{2+}, Ni^{2+}, Zn^{2+}, Cd^{2+}, and Ag^{+}) showed no significant or little effect on the luminescent intensity of the initial EuCP microspheres. The quantified values of the quenching effect of various metal ions were obtained using the Stern-Volmer equation. The quenching effect coefficient K_{sv} value for Cu^{2+} ions at 12,485 M^{-1} was the largest and most distinguishable among those of other metal ions (Supplementary Table S1).

Reducing the amount of sensing-active EuCP materials. The small size of EuCP microspheres in comparison to that of typical macro-scaled MOF-based sensing materials is an excellent advantage in terms of the effective sensing event, because the luminescent signal of sensing materials is significantly contributed from the exterior of

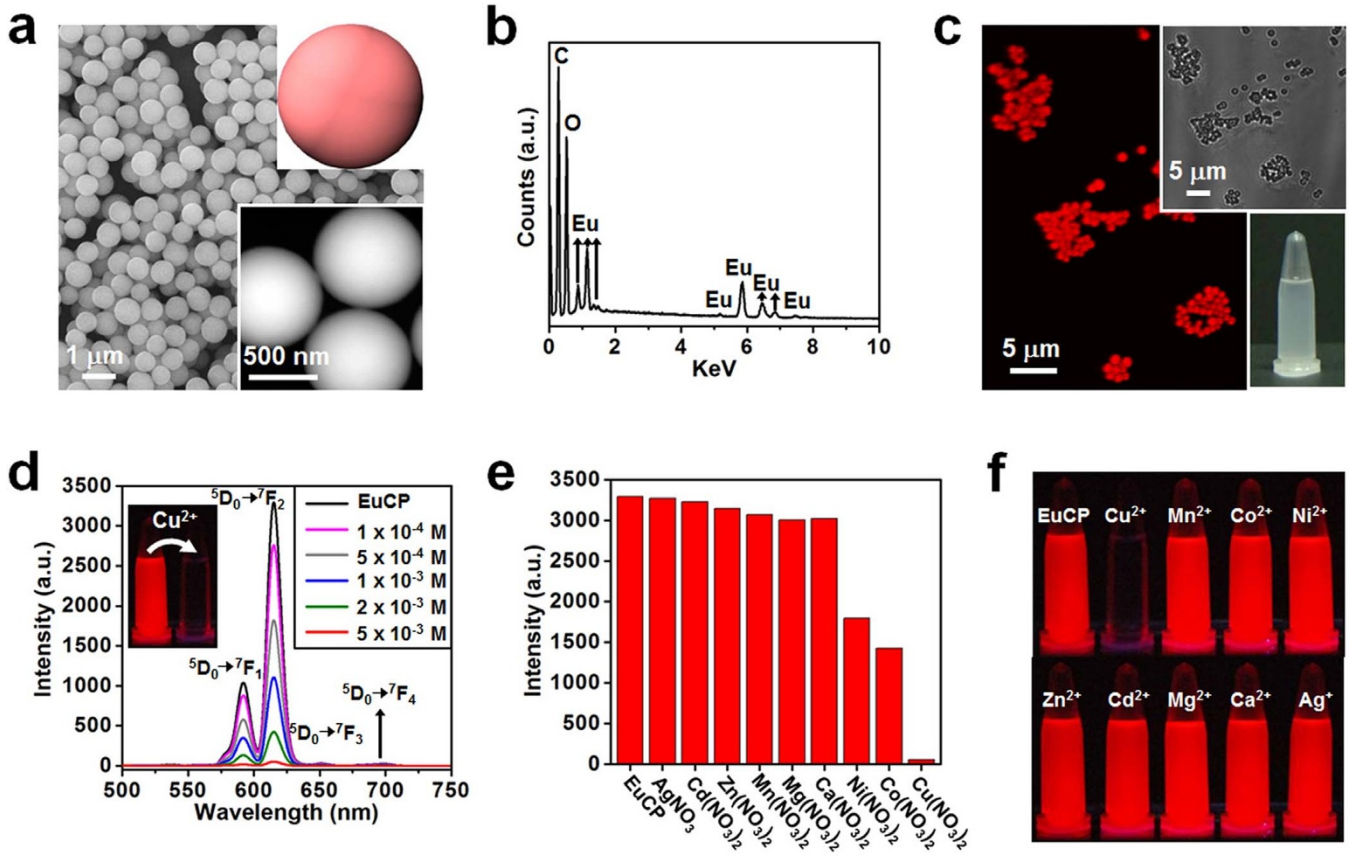

Figure 2 | Morphology, optical property, and sensing property of EuCP microspheres. (a) SEM and STEM (inset) images of europium(III) coordination polymer (EuCP) microspheres (0.70 ± 0.06 μm, s.d., n = 100). (b) EDX spectrum and (c) confocal microscopy and OM (top inset) images of EuCP microspheres. Bottom inset in (c) shows EuCP microspheres dispersed in MeCN. (d) Luminescent titration spectra of EuCP microspheres with the addition of various concentrations of $Cu(NO_3)_2$ in MeCN with an excitation wavelength of 280 nm. Inset in (d) shows the EuCP microspheres suspension before and after immersion in a Cu^{2+} solution with UV irradiation. (e) Luminescent intensity changes of EuCP microspheres after immersion in various metal ion solutions (5 mM). (f) Photograph of a series of EuCP microspheres suspensions before and after immersion in various metal ion solutions in the presence of UV irradiation.

the materials, with only an insignificant contribution coming from the interior of the materials. The internal portion of the sensor materials is not seriously necessary for the sensing event, and so core-shell type sensing materials with the sensing-active shell will be still good enough for the effective sensing event. Core-shell type sensor materials will result in reducing the amount of required sensor materials and decrease waste. Luminescent silica@EuCP core-shell microspheres[31] were prepared according to the reported solvothermal method[31,32] (Fig. 1). The reaction of carboxylic acid-terminated silica particles with coordination polymer precursors of $Eu(NO_3)_3$ and H_2IPA at 140°C for 20 min resulted in the formation of uniform silica@EuCP microspheres. The resulting monodisperse silica@EuCP was first identified by SEM and STEM, as shown in Fig. 3a,b. Microscopy images clearly showed the formation of uniform microspheres and a size increase from 0.87 ± 0.02 μm for bare silica particles to 1.10 ± 0.03 μm after

Table 1 | Synthetic times, used amounts, and sensitivities of selected lanthanide(III)-based luminescent solid sensors

Entry	lanthanide(III)-based solid sensors*	Synthetic time	Amount of sensors used†	K_{sv}‡ [M^{-1}]	ref
1	EuMOF (PDC)	24 h	5 mg	89	10
2	EuMOF (FMA & OX)	48 h	10 mg	529	9
3	EuMOF (FBPT)	48 h	1 mg	2,470§	12
4	EuMOF (BPT)	24 h	1 mg	6,637§	8
5	EuMOF (BPYDB)	72 h	NA	280§	13
6	TbMOF (BPDC & BPDCA)	72 h	~4 mg	345	11
7	EuCP (IPA)	0.33 h	0.1 mg	12,485	this work
8	silica@EuCP (IPA)	0.33 h	0.1 mg (0.06 mg)	15,200	this work
9	silica@TbCP (IPA)	0.33 h	0.1 mg (0.06 mg)	30,763	this work
10	thin silica@TbCP (IPA)	0.33 h	0.1 mg (0.026 mg)	36,432	this work
11	thin silica@TbCP (IPA)	0.33 h	0.01 mg (0.0026 mg)	39,069	this work

*Indicated identity of lanthanide ions and organic ligands within solid sensors; PDC = pyridine-3,5-dicarboxylate, FMA = fumarate, OX = oxalate, FBPT = 2′-fluoro-biphenyl-3,4′,5-tricarboxylate, BPT = biphenyl-3,4′,5-tricarboxylate, BPYDB = 4,4′-(4,4′-bipyridine-2,6-diyl) dibenzoate, BPDC = 3,3′-dicarboxylate-2,2′-dipyridine, BPDCA = biphenyl-4,4′-dicarboxylate, and IPA = isophthalate. †Amount of sensors used per 1 mL solvent. Numbers in blankets mean the actual amounts of LnCP within silica@LnCP structures. ‡Calculated from the Stern-Volmer equation ($I_0/I = 1 + K_{sv}[M]$). §Calculated from the data provided in references.

the formation of silica@EuCP. The thickness of the coordination polymer shell (EuCP) was 115 nm. Specially, the STEM image clearly showed the formation of well-organized core-shell structure. The relative weight percentages of both EuCP shell and silica core within silica@EuCP were calculated at *ca.* 6 : 4 (w/w, EuCP : silica). The relative weight percentages of EuCP shell and silica core were obtained by measuring the weight of the samples before and after removing the EuCP shell from the silica@EuCP using acetic acid. The formation of silica@EuCP core-shell structures was further verified using energy dispersive X-ray (EDX) spectroscopy, EDX spectrum profile scanning, IR spectroscopy, and PXRD (Fig. 3c,d, Supplementary Fig. S1, and Supplementary Fig. S2). Especially, EDX spectrum profile scanning of silica@EuCP revealed the characteristic features for core-shell structure, where silica atoms were dominant at the center of the particles and europium atoms were abundant at the edge of the particles as a component of the shell (Fig. 3d). Confocal microscopy image (Fig. 3e) and photograph with UV irradiation (shown on the left side of Fig. 3h) of silica@EuCP microspheres visually showed luminescence in red regions of the spectrum due to the luminescent EuCP shell.

Selective Cu^{2+} sensing of luminescent silica@EuCP microspheres. A study was conducted on the utilization of core-shell type silica@

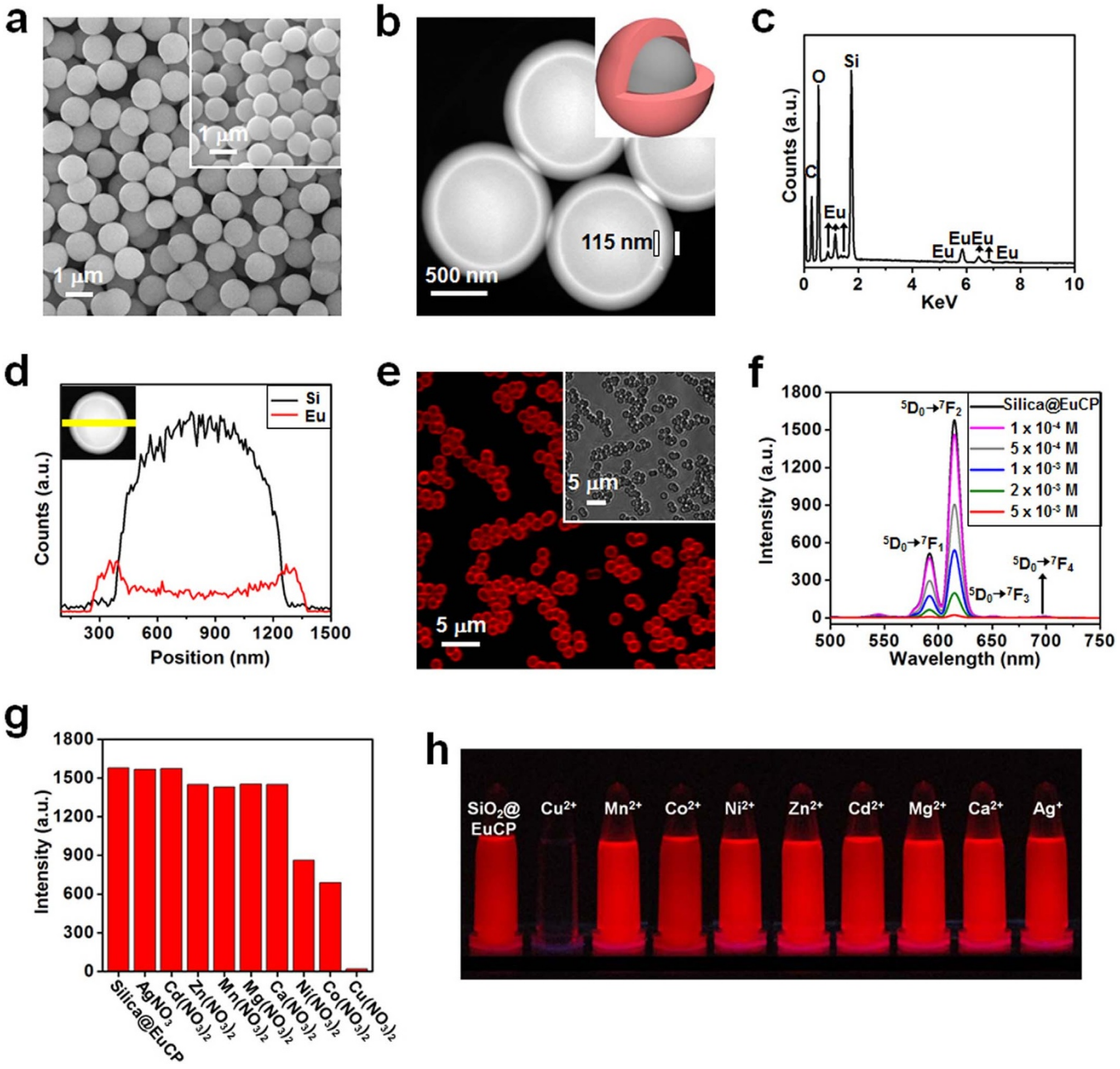

Figure 3 | Morphology, optical property, and sensing property of silica@EuCP microspheres. (a) SEM and (b) STEM images of silica@EuCP microspheres (1.10 ± 0.03 μm). SEM image of initial silica (0.87 ± 0.02 μm) are shown in insets of (a) (s.d., $n = 100$). (c) EDX spectrum, (d) EDX spectrum profile scanning, and (e) confocal microscopy and OM (inset) images of silica@EuCP microspheres. (f) Luminescent titration spectra of silica@EuCP microspheres with the addition of various concentrations of $Cu(NO_3)_2$ in MeCN with an excitation wavelength of 280 nm. (g) Luminescent intensity changes of silica@EuCP microspheres after immersion in various metal ion solutions (5 mM). (h) Photograph of a series of silica@EuCP microspheres suspensions before and after immersion in various metal ion solutions in the presence of UV irradiation.

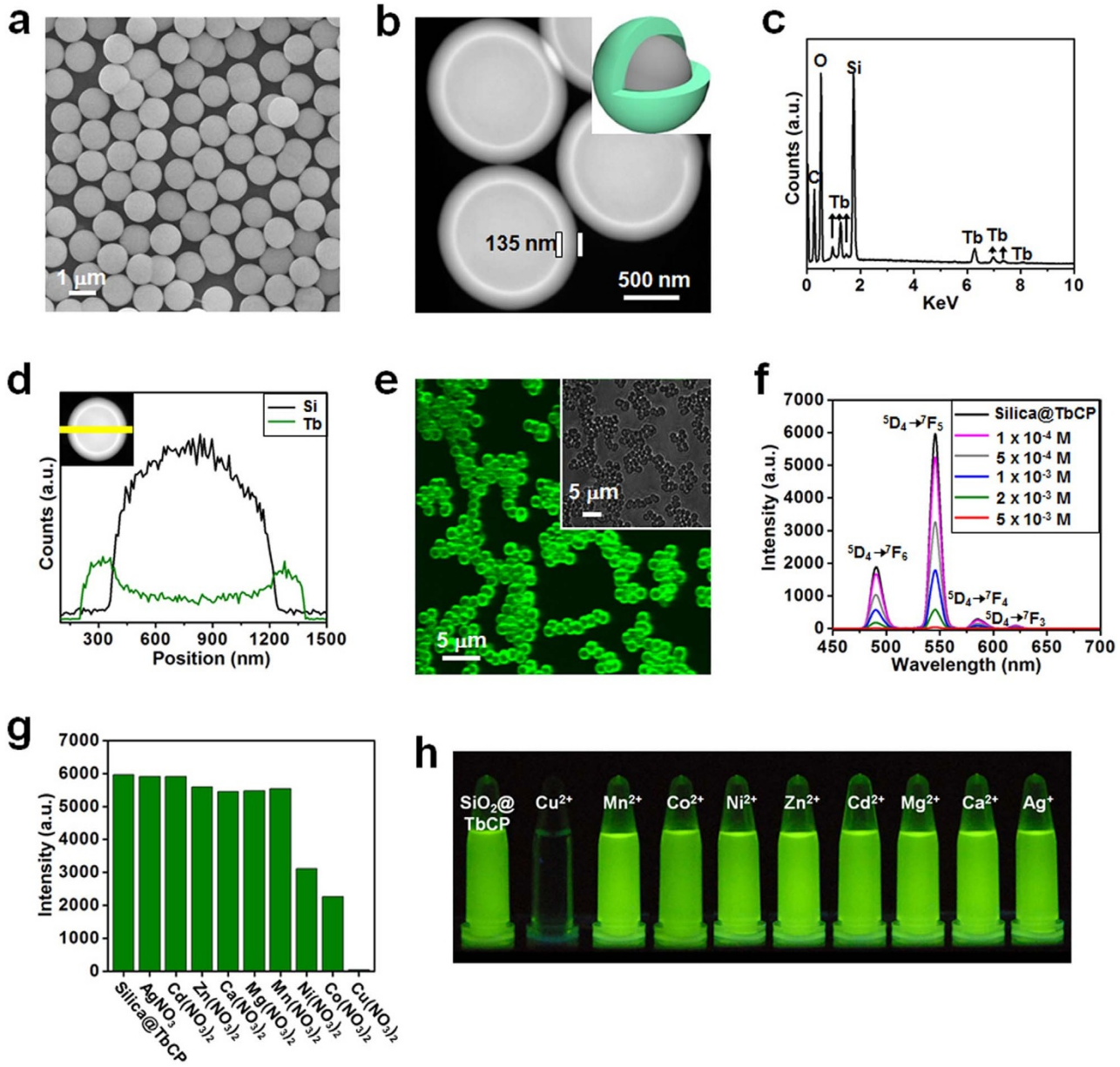

Figure 4 | Morphology, optical property, and sensing property of silica@TbCP microspheres. (a) SEM and (b) STEM images of silica@TbCP microspheres (1.14 ± 0.02 μm, s.d., $n = 100$). (c) EDX spectrum, (d) EDX spectrum profile scanning, and (e) confocal microscopy and OM (inset) images of silica@TbCP microspheres. (f) Luminescent titration spectra of silica@TbCP microspheres with the addition of various concentrations of $Cu(NO_3)_2$ in MeCN with an excitation wavelength of 280 nm. (g) Luminescent intensity changes of silica@TbCP microspheres after immersion in various metal ions solutions (5 mM). (h) Photograph of a series of silica@TbCP microspheres suspensions before and after immersion in various metal ion solutions in the presence of UV irradiation.

EuCP microspheres as a luminescent sensor along with the EuCP microspheres. The sensitivity of silica@EuCP core-shell in Cu^{2+} sensing was nearly identical with that of the pure EuCP microspheres, as shown in the titration of an MeCN suspension of silica@EuCP microspheres with various concentrations of Cu^{2+} (Fig. 3f). The turn-off signal of the silica@EuCP microspheres upon the Cu^{2+} addition was easily identified by the naked eye, as shown in Fig. 3h. The sensing selectivity of silica@EuCP microspheres was also essentially identical to that of pure EuCP microspheres, as shown in the series of the luminescent intensity changes after immersion in various kinds of metal ion solutions (Fig. 3g,h, and Supplementary Table S2). The K_{sv} value (15,200 M^{-1}) for Cu^{2+} ions of silica@EuCP is *ca.* 20% higher than that of pure EuCP microspheres (12,485 M^{-1}). As demonstrated here, though the amount of EuCP within silica@EuCP microspheres was reduced to *ca.* 60% in comparison to pure EuCP microspheres, the sensitivity and selectivity of silica@EuCP core-shell for metal ion sensing does not decrease.

Silica@TbCP microspheres as highly effective solid sensor. Analogue silica@TbCP core-shell microspheres were also synthesized from a similar solvothermal reaction of carboxylic acid-terminated silica particles with $Tb(NO_3)_3$ and H_2IPA at 140°C for 20 min. The formation of uniform silica@TbCP microspheres was first identified by SEM and STEM images. Microscopy images (Fig. 4a,b) revealed the formation of uniform core-shell structure with an average size of 1.14 ± 0.02 μm and TbCP shell thickness of 135 nm. The EDX spectrum and EDX spectrum profile scanning confirmed its chemical compositions (Fig. 4c,d). The emission spectrum of silica@TbCP microspheres showed the characteristic transitions of Tb^{3+} ions (Fig. 4f). The strong emission bands at 491 and 546 nm are attributed to the $^5D_4 \rightarrow$

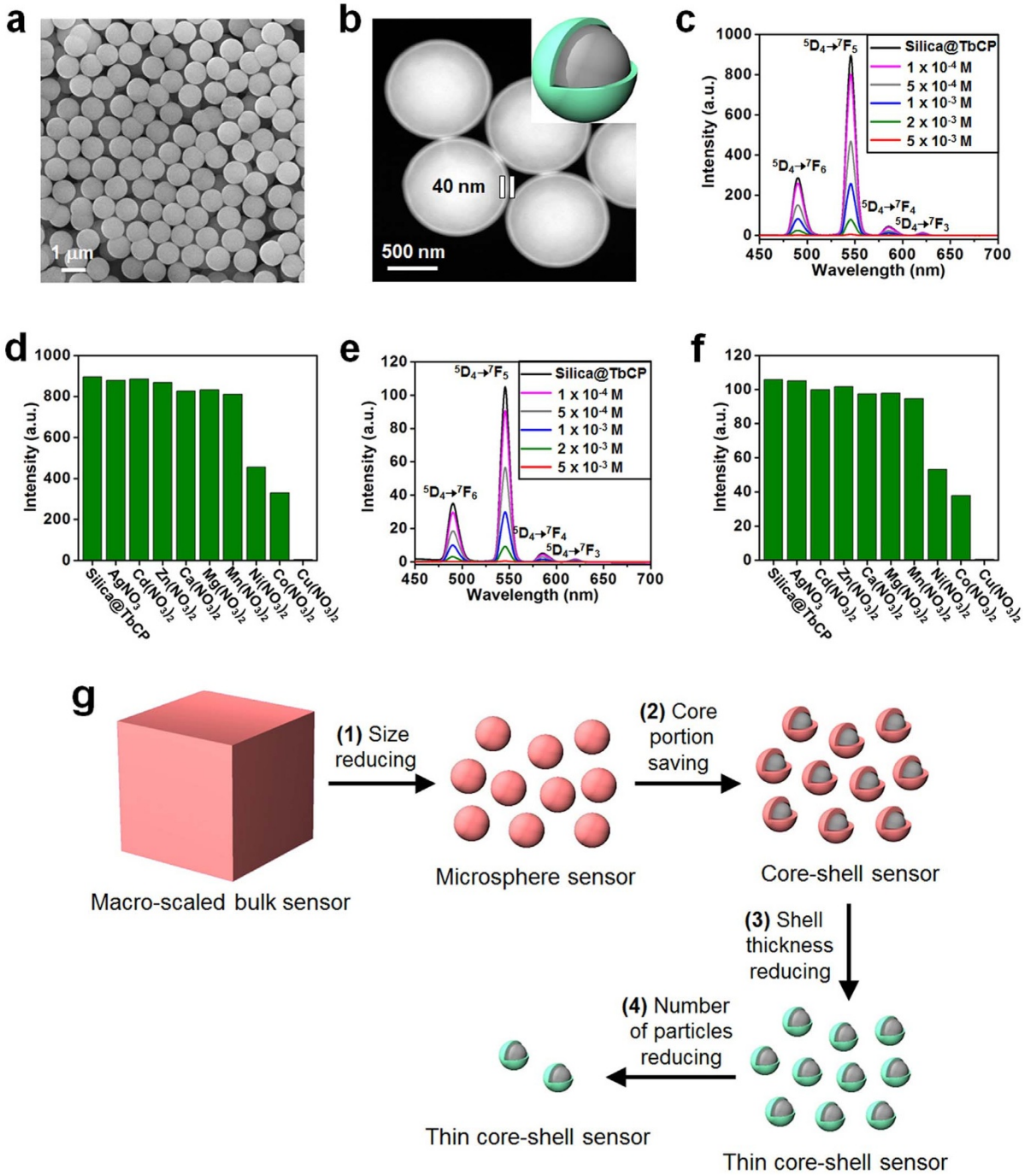

Figure 5 | Ideal heterogeneous solid sensor with small size and thin sensing-active layer. (a) SEM and (b) STEM images of thin silica@TbCP microspheres (0.95 ± 0.02 μm, s.d., $n = 100$). (c) Luminescent titration spectra of thin silica@TbCP microspheres (0.1 mg) with the addition of various concentrations of $Cu(NO_3)_2$ in MeCN. Excitation wavelength was 280 nm. (d) Luminescent intensity changes of thin silica@TbCP microspheres (0.1 mg) after immersion in various metal ions solutions (5 mM). (e) Luminescent titration spectra in the presence of small amount of thin silica@TbCP microspheres (0.01 mg) with the addition of various concentrations of $Cu(NO_3)_2$ in MeCN. (f) Luminescent intensity changes of small amount of thin silica@TbCP microspheres (0.01 mg) after immersion in various metal ions solutions (5 mM). (g) Schematic representation outlining the strategy for design of ideal heterogeneous sensor particles (reducing the amount of required sensor material).

$^7F_6$ and $^5D_4 \rightarrow {}^7F_5$ transitions of Tb^{3+} ions, respectively[11,14]. These intense transitions resulted in the green emission of particles. Confocal microscopy image (Fig. 4e) and photograph (far left in Fig. 4h) in the presence of UV irradiation of silica@TbCP microspheres visually showed luminescence in green regions of the spectrum. Weak emission bands at 585 and 621 nm originating from the $^5D_4 \rightarrow {}^7F_4$ and $^5D_4 \rightarrow {}^7F_3$ transitions were also observed in the emission spectrum of the silica@TbCP microspheres.

The initial luminescent intensity of silica@TbCP microspheres was much stronger than that of silica@EuCP microspheres (Fig. 4f). In addition, the silica@TbCP exhibited superior sensing sensitivity in Cu^{2+} detection over silica@EuCP, as shown in the titration of the MeCN suspension of silica@TbCP microspheres with various concentrations of Cu^{2+} (Fig. 4f). The K_{sv} value for Cu^{2+} ions of silica@TbCP microspheres was 30,763 M^{-1}. The sensitivity of silica@TbCP on Cu^{2+} detecting was 2 times higher than that of

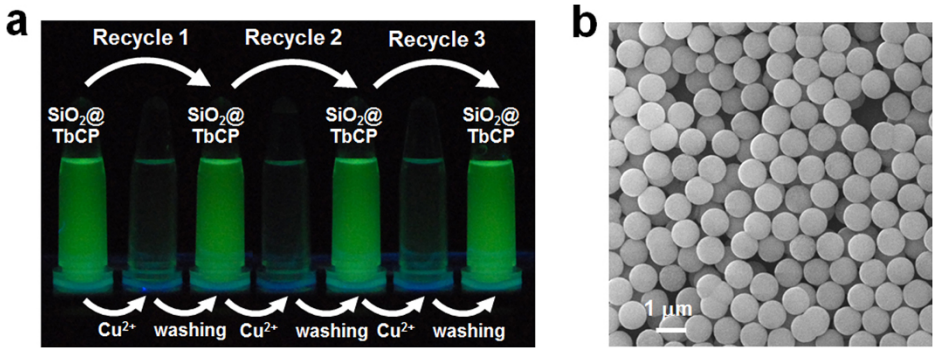

Figure 6 | Recycling of thin silica@TbCP sensors. (a) Photograph of a series of thin silica@TbCP microspheres recycled 3 times for Cu^{2+} sensing. (b) An SEM image of thin silica@TbCP microspheres following the 3rd recycle.

silica@EuCP. Turn-off sensing of silica@TbCP on Cu^{2+} was also easily identified by the clear disappearance of the green emission of silica@TbCP after immersion in Cu^{2+} solution (Fig. 4h). The sensing selectivity of silica@TbCP microspheres was also similar to that of silica@EuCP microspheres, as shown in the luminescent intensity changes attributed to various metal ions (Fig. 4g,h, Supplementary Fig. S5a, and Supplementary Table S3).

Reducing sensing-active TbCP shell thickness. The portion of the coordination polymers responsible for signalling within the core-shell sensor materials can be additionally reduced by decreasing the coordination polymer shell thickness. Thin silica@TbCP microspheres with an average thickness of 40 nm were prepared from a similar solvothermal reaction, but with a decreased amount of coordination polymer precursors to that used during core-shell formation while maintaining the same amount of silica cores (Fig. 5a,b, and Supplementary Fig. S6). In this case, the weight ratio between the luminescent TbCP shell and silica core was only *ca.* 1 : 3 (w/w, TbCP : silica). The sensitivity (Fig. 5c) and selectivity (Fig. 5d and Supplementary Table S4) on Cu^{2+} sensing of thin silica@TbCP microspheres was unchanged, even after reducing the shell thickness of the luminescent TbCP. The K_{sv} value for Cu^{2+} ions of thin silica@TbCP microspheres (36,432 M^{-1}) was slightly higher than thick silica@TbCP microspheres. The sensitivity of thin silica@TbCP microspheres showed an improvement in excess of 550% in comparison to several known LnMOF-based sensor materials (Table 1). Finally, when we used only 0.01 mg of thin silca@TbCP microspheres instead of 0.1 mg, we still achieved a reliable response for the sensing events, as shown in Fig. 5e,f. Only 0.0026 mg of TbCP was presenting within 0.01 mg of thin silica@TbCP, and this miniscule amount of TbCP was sufficient for exceptionally sensitive (more than 550% improvement) and selective sensing of Cu^{2+}. Note that this tiny amount of TbCP (0.0026 mg) is only *ca.* 1/400 ~ 1/4000 of the quantity of other known MOF-based sensors, where 1 ~ 10 mg of MOF-based sensors were used during the sensing events.

Recyclability of silica@TbCP micro-sensors. In last, we have demonstrated the recyclability of thin silica@TbCP microspheres for sensing processes. Silica@TbCP microspheres can be reused several times by simply washing the micro-sensors with fresh MeCN after the sensing process (Fig. 6a). SEM image of thin silica@TbCP microspheres measured after 3 successive usages was shown in Fig. 6b.

Discussion

In summary, we have developed highly effective heterogeneous sensor materials based upon luminescent coordination polymers. The small size and excellent dispersity of micro-sized EuCP spheres make it possible for extremely sensitive and selective sensing on Cu^{2+} ions. Interestingly, small amounts of EuCP microspheres were sufficient for a reliable sensing process. The amount of sensor materials (EuCP) can be further reduced by making sensor in the form of core-shell, and so cutting off the waste. Core-shell type silica@LnCP microspheres showed the enhanced sensing sensitivity. The amount of sensor materials (LnCP) was additionally reduced by decreasing the shell thickness of the luminescent LnCP within silica@LnCP microspheres. The sensitivity of thin silica@TbCP microspheres, which contain tiny amount of sensing active materials, exhibited an improvement more than 550% in comparison to known LnMOF-based sensor materials. Finally, we found that only 0.0026 mg of luminescent LnCP, which is *ca.* 1/400 ~1/4000 of amount of MOF-based sensors typically required in sensing events, was sufficient for a reliable sensing event. Reducing the size of solid sensor and producing well-structured core-shells from solid sensing materials are an ideal direction for the future heterogeneous sensor development (Fig. 5g). In addition, the resulting micro-sized core-shell sensor exhibited the excellent recyclability.

Methods

General Methods. Solvents and all other chemicals were obtained from commercial sources and were used as received unless otherwise noted. Carboxylic acid-terminated silica particles were purchased from Polysciences, Inc. (USA). All scanning electron microscopy (SEM) images were obtained using a JEOL JSM-7001F field-emission SEM, and energy dispersive X-ray (EDX) spectra were obtained using a Hitachi SU 1510 SEM equipped with a Horiba EMAX Energy E-250 EDS system. All scanning transmission electron microscopy (STEM) images were obtained using an FEI Tecnai G2 F30 ST and were carried out using dark-field imaging in STEM mode at 300 kV, and EDX spectrum profile scanning data were obtained using an STEM attachment at Korea Basic Science Institute Seoul Center. Luminescent properties were measured on a Jasco FP-8500 fluorometer using quartz cells (10 × 4 mm light path). All confocal microscopy images were obtained using a Multiphoton CLSM (LSM 780 NLO, GaAsP detector, Carl-Zeiss) with a Ti:Sappuire laser (Maitai eHP deepsee, Spectra Physics) at Korea Basic Science Institute Chuncheon Center. The infrared spectra of solid samples were obtained on a Jasco FT/IR-4200 spectrometer. X-ray diffraction patterns were conducted using a Rigaku Ultima IV equipped with a graphite-monochromated $Cu_{k\alpha}$ radiation source (40 kV, 40 mA). Thermogravimetric analysis (TGA) measurements were carried out using a Shimadzu TGA-50 in a nitrogen atmosphere at a heating rate of 10°C min^{-1}.

Preparation of luminescent EuCP microspheres. A coordination polymer precursor solution was prepared by mixing isophthalic acid (H_2IPA, 10.0 mg, 0.060 mmol) and $Eu(NO_3)_3 \cdot 5H_2O$ (28.4 mg, 0.066 mmol) in 15 mL of DMF/THF cosolvent (2 : 1, v/v). The resulting precursor solution was placed in an oil bath (140 °C). After 20 minutes, resulting spherical particles were isolated and subsequently washed with DMF and MeCN *via* centrifugation-redispersion cycles. Each successive supernatant was decanted and replaced with fresh solvent. IR for EuCP microspheres (KBr): 1606s, 1540s, 1481m, 1446m, 1402s, 1316w, 1280w, 1165w, 1106w, 1078w, 1003w, 927w, 874w, 833w, 811w, 747m, 717m, 681w, 658w, 636w, 626w, 610w, 579w, 534w, 472w.

Preparation of luminescent silica@LnCP (Ln = Eu or Tb) microspheres. A coordination polymer precursor solution was prepared by mixing isophthalic acid (H_2IPA, 8.0 mg, 0.048 mmol) and $Eu(NO_3)_3 \cdot 5H_2O$ (22.7 mg, 0.053 mmol) in 12 mL of DMF/THF cosolvent (2 : 1, v/v). The precursor solution was then mixed with carboxylic acid-terminated silica (12.0 mg). The resulting mixture was placed in

an oil bath at 140 °C for 20 min. Luminescent silica@EuCP core-shell microspheres generated during this time were isolated by cooling the reaction mixture to room temperature, collecting the precipitate through centrifugation, and washing the precipitate several times with DMF and MeCN. Each successive supernatant was decanted and replaced with fresh solvent. Luminescent silica@TbCP microspheres were also prepared using $Tb(NO_3)_3 \cdot 5H_2O$, under otherwise identical reaction conditions to those described above. IR for silica@EuCP microspheres (KBr): 1607s, 1543s, 1481m, 1447m, 1399s, 1316w, 1277w, 1104s, 943w, 875w, 801w, 747m, 716m, 657w, 635w, 472s. IR for silica@TbCP microspheres (KBr): 1607s, 1543s, 1481m, 1449m, 1400s, 1315w, 1277w, 1104s, 949w, 874w, 810w, 747m, 717m, 658w, 628w, 472s.

Preparation of thin silica@TbCP microspheres. Silica@TbCP microspheres with thin TbCP shell thickness was prepared by using small amounts of coordination polymer precursors (H_2IPA; 2.0 mg, $Tb(NO_3)_3 \cdot 5H_2O$; 5.76 mg) and same amount of carboxylic acid-terminated silica particles (12.0 mg), under otherwise identical reaction conditions to those described above.

Measurements of luminescent properties. The luminescent properties of samples (spherical and core-shell microspheres) were measured in MeCN suspensions at room temperature. The luminescent titration spectra were measured by immersing EuCP microspheres or silica@LnCP microspheres (0.1 mg or 0.01 mg) into MeCN solutions (1.0 mL) of various concentrations of $Cu(NO_3)_2$ (0.1 mM ~ 5 mM). For the sensing selectivity experiments, EuCP microspheres or silica@LnCP microspheres (0.1 mg or 0.01 mg) were immersed in MeCN solutions (1.0 mL) containing $M(NO_3)_2$ ($M = Mg^{2+}$, Ca^{2+}, Mn^{2+}, Co^{2+}, Ni^{2+}, Cu^{2+}, Zn^{2+}, Cd^{2+}) or $AgNO_3$ with a concentration of 5 mM. For recycling, the used silica@TbCP microspheres were washed several times with fresh MeCN.

1. Gaggelli, E., Kozlowski, H., Valensin, D. & Valensin, G. Copper homeostasis and neurodegenerative disorders (Alzheimer's, Prion, and Parkinson's diseases and amyotrophic lateral sclerosis). *Chem. Rev.* **106**, 1995–2044 (2006).
2. Barnham, K. J., Masters, C. L. & Bush, A. I. Neurodegenerative diseases and oxidative stress. *Nat. Rev. Drug Discov.* **3**, 205–214 (2004).
3. Brunner, J. & Kraemer, R. Copper(II)-quenched oligonucleotide probes for fluorescent DNA sensing. *J. Am. Chem. Soc.* **126**, 13626–13627 (2004).
4. Choi, J. K. *et al.* A PCT-based, pyrene-armed calix[4]crown fluoroionophore. *J. Org. Chem.* **71**, 8011–8015 (2006).
5. Mu, L., Shi, W., Chang, J. C. & Lee, S.-T. Silicon nanowires-based fluorescence sensor for Cu(II). *Nano Lett.* **8**, 104–109 (2008).
6. Jayaramulu, K., Narayanan, R. P., George, S. J. & Maji, T. K. Luminescent microporous metal-organic framework with functional Lewis basic sites on the pore surface: specific sensing and removal of metal ions. *Inorg. Chem.* **51**, 10089–10091 (2012).
7. Kreno, L. E. *et al.* Metal-organic framework materials as chemical sensors. *Chem. Rev.* **112**, 1105–1125 (2012).
8. Hao, Z. *et al.* A europium(III) based metal-organic framework: bifunctional properties related to sensing and electronic conductivity. *J. Mater. Chem. A* **2**, 237–244 (2014).
9. Xiao, Y. *et al.* A microporous luminescent metal-organic framework for highly selective and sensitive sensing of Cu^{2+} in aqueous solution. *Chem. Commun.* **46**, 5503–5505 (2010).
10. Chen, B. *et al.* A luminescent metal-organic framework with Lewis basic pyridyl sites for the sensing of metal ions. *Angew. Chem. Int. Ed.* **48**, 500–503 (2009).
11. Zhou, J.-M., Shi, W., Li, H.-M., Li, H. & Cheng, P. Experimental studies and mechanism analysis of high-sensitivity luminescent sensing of pollutional small molecules and ions in Ln_4O_4 cluster based microporous metal-organic frameworks. *J. Phys. Chem. C* **118**, 416–426 (2014).
12. Hao, Z. *et al.* One-dimensional channel-structured Eu-MOF for sensing small organic molecules and Cu^{2+} ion. *J. Mater. Chem. A* **1**, 11043–11050 (2013).
13. Song, X.-Z. *et al.* Single-crystal-to-single-crystal transformation of a europium(III) metal-organic framework producing a multi-responsive luminescent sensor. *Adv. Funct. Mater.* **24**, 4034–4041 (2014).
14. Yang, W. *et al.* MOF-76: from a luminescent probe to highly efficient U^{VI} sorption material. *Chem. Commun.* **49**, 10415–10417 (2013).
15. Chen, B., Wang, L., Zapata, F., Qian, G. & Lobkovsky, E. B. A luminescent microporous metal-organic framework for the recognition and sensing of anions. *J. Am. Chem. Soc.* **130**, 6718–6719 (2008).
16. Chen, B. *et al.* Luminescent open metal sites within a metal-organic framework for sensing small molecules. *Adv. Mater.* **19**, 1693–1696 (2007).
17. Dincă, M. *et al.* Observation of Cu^{2+}-H_2 interactions in a fully desolvated sodalite-type metal-organic framework. *Angew. Chem. Int. Ed.* **46**, 1419–1422 (2007).
18. Wang, B., Côté, A. P., Furukawa, H., O'Keeffe, M. & Yaghi, O. M. Colossal cages in zeolitic imidazolate frameworks as selective carbon dioxide reservoirs. *Nature* **453**, 207–211 (2008).
19. Huang, A. & Caro, J. Covalent post-functionalization of zeolitic imidazolate framework ZIF-90 membrane for enhanced hydrogen selectivity. *Angew. Chem. Int. Ed.* **50**, 4979–4982 (2011).
20. Yanai, N. *et al.* Gas detection by structural variations of fluorescent guest molecules in a flexible porous coordination polymer. *Nat. Mater.* **10**, 787–793 (2011).
21. Bohnsack, A. M., Ibarra, I. A., Bakhmutov, V. I., Lynch, V. M. & Humphrey, S. M. Rational design of porous coordination polymers based on bis(phosphine)MCl_2 complexes that exhibit high-temperature H_2 sorption and chemical reactivity. *J. Am. Chem. Soc.* **135**, 16038–16041 (2013).
22. Tanabe, K. K. & Cohen, S. M. Engineering a metal-organic framework catalyst by using postsynthetic modification. *Angew. Chem. Int. Ed.* **48**, 7424–7427 (2009).
23. Zhu, Q.-L. & Xu, Q. Metal-organic framework composites. *Chem. Soc. Rev.* **43**, 5468–5512 (2014).
24. Aijaz, A., Akita, T., Tsumori, N. & Xu, Q. Metal-organic framework-immobilized polyhedral metal nanocrystals: reduction at solid-gas interface, metal segregation, core-shell structure, and high catalytic activity. *J. Am. Chem. Soc.* **135**, 16356–16359 (2013).
25. Oh, M. & Mirkin, C. A. Chemically tailorable colloidal particles from infinite coordination polymers. *Nature* **438**, 651–654 (2005).
26. Lee, H. J., Cho, Y. J., Cho, W. & Oh, M. Controlled isotropic or anisotropic nanoscale growth of coordination polymers: formation of hybrid coordination polymer particles. *ACS Nano* **7**, 491–499 (2013).
27. Cho, W., Lee, H. J. & Oh, M. Growth-controlled formation of porous coordination polymer particles. *J. Am. Chem. Soc.* **130**, 16943–16946 (2008).
28. Li, T., Sullivan, J. E. & Rosi, N. L. Design and preparation of a core-shell metal-organic framework for selective CO_2 capture. *J. Am. Chem. Soc.* **135**, 9984–9987 (2013).
29. Liu, D., Huxford, R. C. & Lin, W. Phosphorescent nanoscale coordination polymers as contrast agents for optical imaging. *Angew. Chem. Int. Ed.* **50**, 3696–3700 (2011).
30. Horcajada, P. *et al.* Porous metal-organic-framework nanoscale carriers as a potential platform for drug delivery and imaging. *Nat. Mater.* **9**, 172–178 (2010).
31. Lee, H. J., Park, J.-U., Choi, S., Son, J. & Oh, M. Synthesis and photoluminescence properties of Eu^{3+}-doped silica@coordination polymer core-shell structures and their calcinated silica@Gd_2O_3:Eu and hollow Gd_2O_3:Eu microsphere products *Small* **9**, 561–569 (2013).
32. Jo, C., Lee, H. J. & Oh, M. One-pot synthesis of silica@coordination polymer core-shell microspheres with controlled shell thickness *Adv. Mater.* **23**, 1716–1719 (2011).

Acknowledgments

This work was supported by the National Leading Research Lab Program (no. NRF-2012R1A2A1A03670409) through NRF grant funded by the Ministry of Science, ICT and Future Planning.

Author contributions

M.O. planned and organized the project, and wrote the paper; W.C., H.J.L., S.C. and Y.K. performed the experiments, and collected data; M.O., W.C., H.J.L., S.C. and Y.K. discussed and analyzed the results.

Additional information

Supplementary information accompanies this paper at http://www.nature.com/scientificreports

Competing financial interests: The authors declare no competing financial interests.

How to cite this article: Cho, W., Lee, H.J., Choi, S., Kim, Y. & Oh, M. Highly effective heterogeneous chemosensors of luminescent silica@coordination polymer core-shell micro-structures for metal ion sensing. *Sci. Rep.* **4**, 6518; DOI:10.1038/srep06518 (2014).